First-Principles Prediction of Electrochemical

Electron-Anion Exchange: Ion-Insertion without

Redox

Daniel L. Druffel,^{†,‡} Jacob T. Pawlik,^{†,‡} Jack D. Sundberg,[†] Lauren M. McRae,[†]
Matthew G. Lanetti,[†] and Scott C. Warren*,[†]

†Department of Chemistry, University of North Carolina at Chapel Hill, Chapel Hill, North

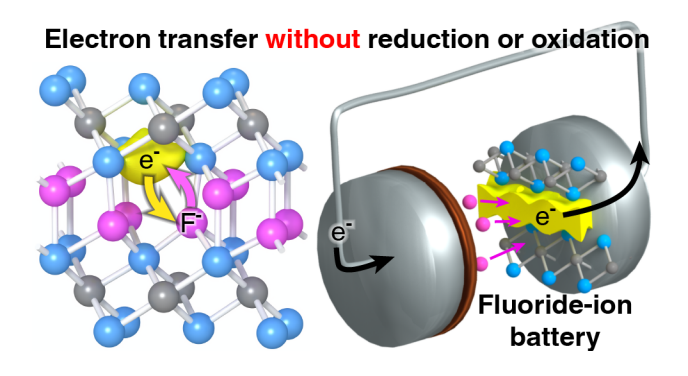
Carolina 27599, United States

‡ These authors contributed equally to this work

E-mail: sw@unc.edu

Abstract

It is widely assumed that the gain or loss of electrons in a material must be accompanied by its reduction or oxidation. Here, we report a system in which the insertion/deinsertion of an electron occurs without any reduction or oxidation. Using first principles methods, we demonstrate this effect in the $Y_2CF_2-[Y_2C]^{2+}(e^-)_2$ material system, where (e^-) indicates a lattice site containing a bare electron. We present a model that when Y_2CF_2 is in contact with a fluoride-containing electrolyte, the application of a positive voltage drives fluorination and a negative voltage reverses the process. We show that this chemistry does not change the oxidation states of the host lattice, causes no significant volume expansion, and occurs rapidly at room temperature. Finally, we demonstrate that this mechanism of ion-insertion may enable a broad class of anion shuttle battery electrodes, some with gravimetric capacities nearly double those employed in intercalation-type Li-ion batteries.



Keywords

electride, battery, anion shuttle, fluorination, defluorination, ion-exchange

An elementary concept of chemistry is that the gain or loss of electrons in a material must be accompanied by the reduction or oxidation of its atoms. Here, we describe an exception to this concept. Some crystalline solids, called electrides, contain lattice sites occupied by a bare electron. These electrons are called "anionic electrons" because they have a charge and size similar to simple anions. The striking parallel between anionic electrons and anions was demonstrated when electrides were reacted with metal halides, producing crystals in which the halide replaced the electride electron with minimal change to the crystal lattice. Despite these findings, the reversible insertion or removal of anions is little explored, perhaps because anion movement typically involves high activation energies. In the following, however, we demonstrate using first principle methods that anions and electrons can be exchanged at room temperature reversibly under electrochemical control (Fig. 1a,b) where the electrode material gains and loses electrons without oxidation or reduction of its atoms.

A natural application of electron-anion exchange (EAX) is in batteries (Fig. 1c). While rapid progress in batteries that shuttle cations between electrodes has led to their widespread use,⁴ batteries that shuttle anions remain largely unexplored. Despite efforts,^{5,6} one deficiency in the science of intercalating anions is the absence of reversible high-capacity elec-

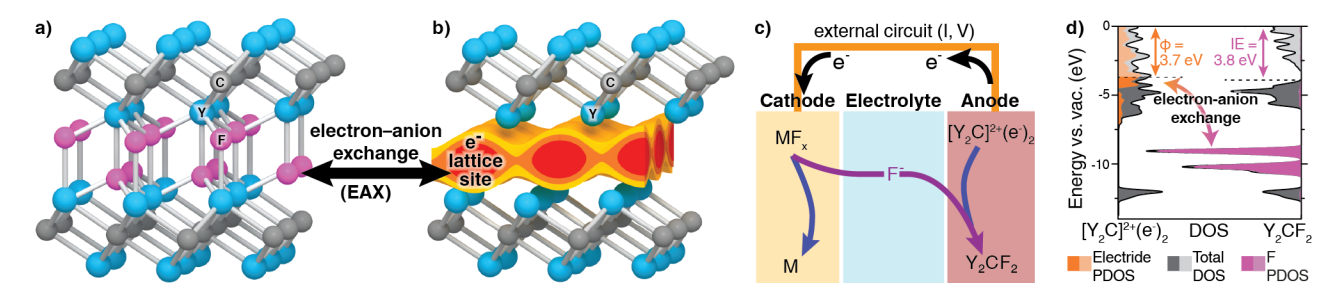


Figure 1: The concept of electron-anion exchange. The reversible conversion of a) Y_2CF_2 to b) $[Y_2C]^{2+}(e^-)_2$ under applied bias where yellow/orange/red show isosurfaces of the anionic electrons at the Fermi level. c) A battery configuration incorporating $[Y_2C]^{2+}(e^-)_2$ as an anode, a F^- electrolyte, and cathode (e.g. a metal fluoride). d) Effect of electron-anion exchange on the partial density of states in the Y_2C system, where IE is the ionization energy and Φ is the work function.

trodes. Here, we show that EAX could enable a broad class of high-capacity electrodes for anion shuttle batteries.

In a general sense, exchanging an anion, such as fluoride, for an electride electron stabilizes the material system because the energetic electride electron shifts onto a lower-lying band comprised of fluorine p orbitals (Fig. 1d). This provides a favorable driving force for a reaction with a fluoride of a less electropositive metal (e.g. Cu) that could act as a cathode in a F⁻ battery. For example, the large free energy of the reaction $[Y_2C]^{2+}(e^-)_2 + CuF_2 \rightarrow Y_2CF_2 + Cu$ suggests a possible cell voltage of 2.8 V (see supporting information). To provide a fundamental grounding for electron-anion exchange, we present computational results that address the oxidation states of the atoms, the mechanism of anion diffusion, and the structural changes that result.

We began by examining the electrides $[Ca_2N]^+e^-$ and $[Sr_2N]^+e^-$, which have positively charged layers of atoms that alternate with negatively charged layers of electrons. We found that fluoride and chloride intercalation were not reversible at room temperature because the corresponding halides are wide band gap insulators with poor ionic mobility. We sought out an isostructural electride, $[Y_2C]^{2+}(e^-)_2$, because our calculations and experiments indicated that the corresponding fluoride, Y_2CF_2 , has a small band gap and high electronic mobility. We expected F^- to intercalate reversibly into the $[Y_2C]^{2+}(e^-)_2$ lattice as the e^- moves into

an external circuit according to the half reaction:

$$[Y_2C]^{2+}(e^-)_2 + 2F^-_{(electrolyte)} \rightleftharpoons [Y_2C]^{2+}(F^-)_2 + 2e^-_{(circuit)}$$
 (1)

For electron-anion exchange to occur at room-temperature, the anionic electron and F^- need to diffuse rapidly through the crystal. To assess F^- movement in the Y₂C system, we modeled a supercell of Y₂CF₂ and removed a fluorine atom, naturally introducing an anionic electron in its place (Fig. 2b). Using density functional theory (DFT) and the nudged elastic band (NEB) method, we calculated a remarkably low activation barrier for electron-fluoride exchange (and thus F^- diffusion) in Y₂CF₂ of only 196 meV (Fig. 2a), which is even lower than the barrier for Li⁺ diffusion in both LiCoO₂ (~300 meV⁸) and graphite (~260 meV⁹). Our calculations reveal that the lowest energy pathway for F^- diffusion in Y₂CF₂ is the F^- hopping directly between tetrahedral sites (Fig. 2b-d), a distance of only 2.44 Å. Because the entire 2D network of sites is accessible by hopping exclusively through tetrahedral sites, we expect that this is the dominant mechanism of F^- diffusion in layered Y₂C system and that F^- diffusion is rapid at room-temperature.

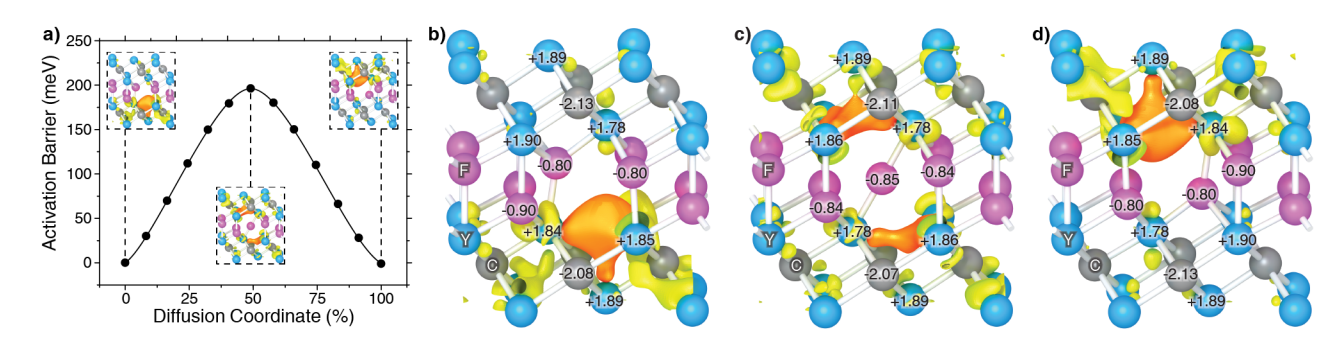


Figure 2: The mechanism of electron-anion exchange. a) The activation barrier for the diffusion of F^- in Y_2CF_2 calculated using the NEB method. b) Electron density isosurfaces near the Fermi level. The ground state of Y_2CF_2 with one F-vacancy showing a F^- (purple) and an anionic electron (orange) at tetrahedral sites prior to exchange. The oxidation states are overlayed on the individual atoms including Y (blue) and carbon (grey). c) The transition state during electron-anion exchange. d) The ground state after the exchange. All e^- densities are plotted at a value of $0.0036 \ e^-/\mathring{A}^3$.

To understand the extent of redox chemistry in electron-anion exchange, we calculated

the oxidation states of the atoms in the host lattice (see supporting information). We find that the oxidation states of Y (1.91+) and C (2.06-) in Y_2CF_2 are nearly identical to those in $[Y_2C]^{2+}(e^-)_2$ (1.95+ and 2.10- respectively) ¹⁰ and also agree with our experimental XPS measurements on Y_2CF_2 that identify a 2+ oxidation state for Y.⁷ Thus, in contrast to traditional ion-insertion chemistry, in which a transition metal changes oxidation state, the net result of EAX is that the atoms in the host lattice are neither reduced nor oxidized.

Though we determined that electron-anion exchange results in no reduction or oxidation overall, a fundamental question remains: whether the elemental step of anion hopping involves transient redox processes in the host lattice. To answer this question, we calculated the electron density as the F⁻ hops along the NEB-path, exchanging sites with an anionic electron (Fig. 2b-d). We find that the position of the anionic electron differs subtly from the position of the F⁻ site (Fig. 2b,d), but the electron density in that site still integrates to 0.8 e⁻ (Table S1). At the transition state, with F⁻ halfway between sites, the anionic electron simultaneously occupies both its initial site and its final site (Fig. 2c). This behavior demonstrates an exciting result: while the anionic electron behaves in many ways like a traditional anion, it can still tunnel in a way common to electrons. We also note that even as the oxidation states remain unchanged (see Table S1), the valence electrons of nearby atoms polarize slightly (Fig. 3). These plots show the change in electron density between the ground state and transition state with red (blue) showing areas that gain (lose) electron density. Individual atoms that surround the moving fluoride gain electron density on one side of the atom but lose electron density on the other, thus leading to a small polarization of the surrounding environment with negligible changes in oxidation state. In addition, bond lengths in the immediate vicinity of the fluoride change less than 0.03 Å, which further highlights how the electron transfer process that occurs in EAX is fundamentally different from ordinary redox processes, which can induce large changes in bond length.

More broadly, the observations about electron-anion exchange highlight similarities to the concept of proton-coupled electron transfer (PCET)¹¹ in which the movement of a pro-

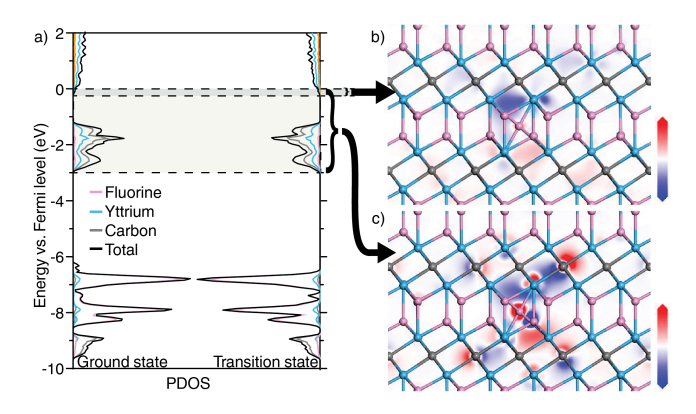


Figure 3: Polarization of valence electrons at and near the Fermi level. a) The partial density of states for the ground and transition states during electron-anion exchange in Y_2CF_2 . b) Electron density deformation plots projected onto a 2D slice along the (110) direction cutting through the anionic electron and hopping F^- . These show the difference in electron density between the transition state and ground state for b) the highest filled bands that comprise the anionic electron and c) the valence bands comprised of the anionic electron, Y, C, and F orbitals, within 2.5 eV of the Fermi level. The scale bars for b and c are, from blue to red, $0.01 \text{ to } 0.01 \text{ e}^-/\text{Å}^3$ and $-0.035 \text{ to } 0.035 \text{ e}^-/\text{Å}^3$, respectively.

ton is coupled to the movement of an electron. Here, our calculations show that anion movement occurs simultaneously with electron movement. We therefore introduce the term anion-coupled electron transfer (ACET) to describe the fundamental step of electron-anion exchange. In the ACET observed in Fig. 2, the transfer of an electron without reduction or oxidation of atoms indicates that the reorganization energy may be small or neglible.

Typically, intercalation is accompanied by significant volume expansion of the host lattice. For example, the insertion of lithium into graphite increases the number of atoms by 17% and leads to an expansion in the c lattice constant of 10%. However, recently, we synthesized Y_2CF_2 and determined its crystal structure, which we find to be remarkably similar to that of $[Y_2C]^{2+}(e^-)_2$. Complete fluorination (Y_2CF_2) increases the number of atoms in $[Y_2C]^{2+}(e^-)_2$ by 66%, yet results in an expansion in the c lattice constant by only 5.2% (Table 1). Moreover, in the Y_2C system, the a and b lattice constants and intralayer atomic distances all change by less than 1.1% (Table 1). We anticipate that the crystal structure may change stacking sequence upon EAX, just as the stacking sequence changes in LiCoO₂ and graphite upon Li⁺ intercalation (see supporting information, Fig. S2), but without disrupting local

Table 1: Atomic distances in $[Y_2C]^{2+}(e^-)_2^{14}$ and $Y_2CF_2^{7}$ with distances in Å and volume, V, in Å³ as determined experimentally.

	$[Y_2C]^{2+}(e^-)_2$	Y_2CF_2	Difference (%)
a	3.62483	3.6651	1.1
c	17.964	18.8907	5.2
Y-Y	2.493	2.510	0.7
Y-C	3.423	3.431	0.2
V	204.413	219.761	7.5

bonding. Importantly, electron-anion exchange and a lack of redox chemistry facilitates the minimal changes in both volume and the local bonding of the host lattice.

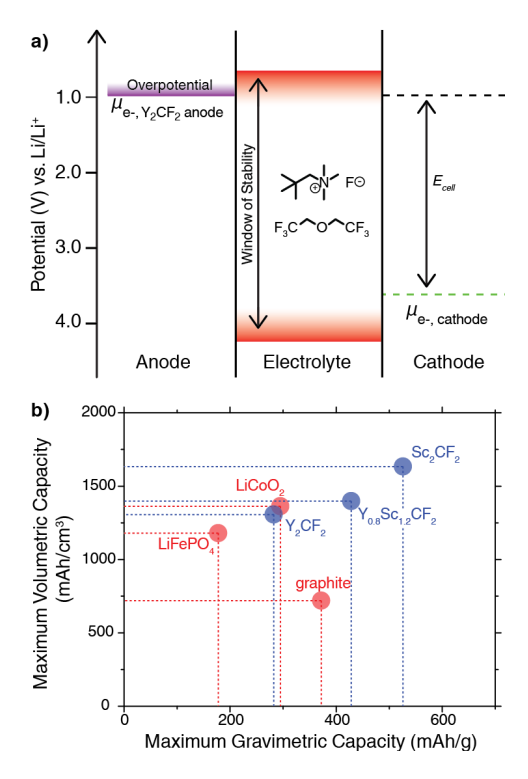


Figure 4: Application of electron-anion exchange a) Potential diagram of a F^- battery utilizing a Y₂CF₂ anode, NpF1/BTFE liquid electrolyte, and a cathode (e.g. CuF₂). b) A comparison of capacities for common Li-ion intercalation electrodes to electrodes that use electron-anion exchange.

Finally, we discuss a natural application of this new mechanism—electrochemical energy storage. We calculated the potential at which electrons insert into Y_2CF_2 to be +0.97 V vs. Li/Li⁺ (Fig. 4a, see supporting information for details), which suggests that $[Y_2C]^{2+}(e^-)_2/Y_2CF_2$ could serve as an anode in a F⁻ battery. The maximum gravimetric

capacity of Y₂CF₂ is a remarkable 282 mAh/g (Fig. 4b), comparable to that of LiCoO₂ (274 mAh/g). ¹⁵ High capacity is achieved despite using the heavy Y atoms because two F⁻ insert into each unit cell of [Y₂C]²⁺(e⁻)₂. Therefore, the gravimetric capacity can be improved by using lighter elements, for example by alloying Y with Sc. ¹⁶ By replacing Y with Sc entirely as in Sc₂CF₂, the density can reach 526 mAh/g, over 70% more than that of LiCoO₂. Sc₂CF₂ also offers a high maximum volumetric capacity reaching 1634 mAh/cm³ (Fig. 4b). Calculations on the Sc₂CF₂ system reveal a small F⁻ diffusion barrier (~400 meV) and useful electron insertion potential (+1.1 V vs Li/Li⁺), suggesting that electrochemical electron-anion exchange can enable champion anodes for F⁻ batteries.

We are exploring this electrochemistry experimentally in a half-cell configuration with electrodes made of Y_2CF_2 using N,N,N-trimethyl-N-neopentylammonium fluoride (NpF1) dissolved in blends of bis(2,2,2-trifluoroethyl)ether and tetraethylene glycol dimethyl ether. ¹⁷ Our experiments will be reported in a separate publication.

We have demonstrated a fundamentally distinct mechanism of electrochemically controlled ion-insertion in which an electron reversibly inserts into a lattice without redox chemistry. Our calculations show that this occurs with minimal changes to the structure or oxidation states of the atoms. We suggest that electron-anion exchange can address a deficiency in the science and technology of intercalation: the absence of high-capacity electrodes that reversibly intercalate anions. We expect that this mechanism will find use in other applications as well, for example in information processing, catalysis, and energy conversion.

Acknowledgement

S.C.W. acknowledges support of this research by NSF grant DMR-1905294. J.T.P. and J.D.S acknowledge support by the NSF Graduate Research Fellowship under grant DGE-1650114. This work was performed in part at the Chapel Hill Analytical and Nanofabrication Laboratory, CHANL, a member of the North Carolina Research Triangle Nanotechnology

Network, RTNN, which is supported by the National Science Foundation, Grant ECCS-1542015, as part of the National Nanotechnology Coordinated Infrastructure, NNCI.

Supporting Information Available

Additional details regarding the DFT calculations, Y₂C phases, calculations of battery performance metrics, and experimental studies.

References

- (1) Keve, E. T.; Skapski, A. C. Ca₂N: a nitride with a layer structure. *Chem. Comm.* (London) **1966**, 829–830.
- (2) Matsuishi, S.; Toda, Y.; Miyakawa, M.; Hayashi, K.; Kamiya, T.; Hirano, M.; Tanaka, I.; Hosono, H. High-density electron anions in a nanoporous single crystal: [Ca₂₄Al₂₈O₆₄]·4(e⁻). *Science* **2003**, *301*, 626–629.
- (3) Bowman, A.; Mason, P. V.; Gregory, D. H. Heteroanionic Intercalation into Positively Charged Inorganic Hosts: the First Nitride Mixed Halides. Chem. Comm. 2001, 1650– 1657.
- (4) Tarascon, J.-M.; Armand, M. Materials for sustainable energy: a collection of peerreviewed research and review articles from Nature Publishing Group; World Scientific, 2011; pp 171–179.
- (5) Nowroozi, M. A.; Wissel, K.; Rohrer, J.; Munnangi, A. R.; Clemens, O. LaSrMnO₄: Reversible Electrochemical Intercalation of Fluoride Ions in the Context of Fluoride Ion Batteries. *Chem. Mater.* 2017, 29, 3441–3453.
- (6) Mohammad, I.; Witter, R.; Fichtner, M.; Anji Reddy, M. Room-temperature, rechargeable solid-state fluoride-ion batteries. *ACS Appl. Energy Mater.* **2018**, *1*, 4766–4775.

- (7) Druffel, D. L.; Lanetti, M. G.; Sundberg, J. D.; Pawlik, J. T.; Stark, M. S.; Donley, C. L.; McRae, L. M.; Scott, K. M.; Warren, S. C. Synthesis and Electronic Structure of a 3D Crystalline Stack of MXene-Like Sheets. *Chem. Mater.* 2019, 31, 9788–9796.
- (8) Okubo, M.; Tanaka, Y.; Zhou, H.; Kudo, T.; Honma, I. Determination of activation energy for Li ion diffusion in electrodes. *J. Phys. Chem. B* **2009**, *113*, 2840–2847.
- (9) Toyoura, K.; Koyama, Y.; Kuwabara, A.; Oba, F.; Tanaka, I. First-principles approach to chemical diffusion of lithium atoms in a graphite intercalation compound. *Phys. Rev.* B 2008, 78, 214303.
- (10) Zhang, X.; Xiao, Z.; Lei, H.; Toda, Y.; Matsuishi, S.; Kamiya, T.; Ueda, S.; Hosono, H. Two-dimensional transition-metal electride Y₂C. *Chem. Mater.* **2016**, *26*, 6638–6643.
- (11) Huynh, M. H. V.; Meyer, T. J. Proton-coupled electron transfer. Chem. Rev. 2007, 107, 5004–5064.
- (12) Schweidler, S.; de Biasi, L.; Schiele, A.; Hartmann, P.; Brezesinski, T.; Janek, J. Volume changes of graphite anodes revisited: A combined operando X-ray diffraction and in situ pressure analysis study. *J. Phys. Chem. C* **2018**, *122*, 8829–8835.
- (13) Atoji, M.; Kikuchi, M. Crystal structures of cubic and trigonal yttrium hypocarbides: A dimorphically interphased singlecrystal study. J. Chem. Phys. 1969, 51, 3863–3872.
- (14) Maehlen, J. P.; Yartys, V. A.; Hauback, B. C. Structural studies of deuterides of yttrium carbide. *J. Alloys Comp.* **2003**, *351*, 151–157.
- (15) Orman, H.; Wiseman, P. Cobalt (III) lithium oxide, CoLiO₂: structure refinement by powder neutron diffraction. *Acta Crystallogr. C* **1984**, 40, 12–14.
- (16) Park, J.; Hwang, J.-Y.; Lee, K. H.; Kim, S.-G.; Lee, K.; Kim, S. W. Tuning the spin-alignment of interstitial electrons in two-dimensional Y₂C electride via chemical pressure. J. Am. Chem. Soc. 2017, 139, 17277–17280.

(17) Davis, V. K. et al. Room-temperature cycling of metal fluoride electrodes: Liquid electrolytes for high-energy fluoride ion cells. *Science* **2018**, *362*, 1144–1148.